

Revitalize LFP! Ascorbic Acid-Assisted Direct Regeneration of Spent LiFePO₄ for Li-Ion Batteries

Tassadit Ouaneche, Lorenzo Stievano, François Rabuel, Arash Jamali, Claude Guéry, Laure Monconduit, Moulay Tahar Sougrati,* and Nadir Recham*

The increasing demand for lithium-ion batteries (LIBs), primarily driven by the expanding electric vehicle market and the growing need for efficient energy storage, presents both significant opportunities and challenges. The efficient and cost-effective regeneration of spent LIBs is crucial to minimizing environmental impact and fostering a true circular economy for battery materials. Herein, an innovative one-step lithiation process is introduced for spent LiFePO₄ cathodes, conducted in aqueous solution under ambient conditions. This method utilizes readily available and low-cost reagents, including a lithium source and ascorbic acid (vitamin C) as a green reducing agent, offering a substantial advantage over traditional techniques that require

harsh conditions and complex setups. The lithiation reaction proceeds rapidly, producing pure and fully regenerated LFP. This environmentally friendly process was successfully demonstrated at the scale of 18650 cells with electrodes composed entirely of recycled LFP. These cells exhibit excellent electrochemical performance, even after 1000 cycles at 1C rate, comparable to those made with pristine LFP. By providing a sustainable, cost-effective, and easily scalable solution for LFP cathode regeneration, the approach supports the closure of the materials loop, contributing to the sustainable management of LIBs and advancing the shift toward a circular economy.

1. Introduction

Global efforts toward sustainable energy pathways have spurred significant advancements in electric vehicle (EV) technology,^[1–4] with a particular focus on enhancing battery performance. Lithium-ion batteries (LIBs) based on lithium iron phosphate (LiFePO₄, LFP) cathodes have recently gained substantial interest from leading EV manufacturers, including Tesla, Ford, BYD, and CATL. Having successfully commercialized EVs extensively in the Asian market, these companies are now progressively introducing LFP batteries in the Western market. They foresee exponential global growth in the adoption of this technology and are exploring it as a viable alternative to traditional NMC batteries and other

cathode materials due to several compelling properties.^[5] LFP-based LIBs offer several advantages over other cathode chemistries, including superior thermal stability and safety,^[6,7] which significantly mitigate the risks of overheating and fire.^[8] This feature is particularly critical in the context of EVs, where safety is paramount.^[9] Furthermore, LFP is known for its longevity, boasting a higher cycle life which translates into a longer operational lifespan for EVs. Another significant benefit is cost efficiency,^[10] as LFP batteries generally use cheaper and more abundant raw materials compared to NMC batteries, which rely on expensive and rare metals such as cobalt. The strategic adoption of LFP batteries by major manufacturers underscores their potential to transform the market. By balancing cost, safety, and longevity, LFP technology is poised to play a critical role in the future of electric mobility.^[5,11]

Recent studies predict a significant shift in the feedstock from NMC to LFP cathodes, with LFP representing more than 50% of the feedstock supply by 2030.^[12] As a result, the production and demand for LFP batteries are expected to increase exponentially, leading to a substantial stockpile of spent batteries in the coming years. The International Energy Agency projects that EV sales will reach a record of more than 145 million vehicles in service globally by 2030.^[13] Moreover, regulatory frameworks in the EU, US, and China are driving the development of innovative solutions to efficiently manage end-of-life (EOL) LIBs.^[14–18]

The recovery of spent LIBs has attracted growing attention.^[19] Common recycling methods include pyrometallurgy and hydrometallurgy.^[20] Currently, the recycling of spent LFP batteries primarily relies on hydrometallurgical methods,^[21] which involve significant chemical consumption and generate large volumes of wastewater while being energy- and time-intensive.^[22] These limitations render hydrometallurgy less aligned with the goals of

T. Ouaneche, L. Stievano, L. Monconduit, M. T. Sougrati

ICGM

Univ. Montpellier

CNRS

ENSCM

34090 Montpellier, France

E-mail: moulay-tahar.sougrati@umontpellier.fr

T. Ouaneche, F. Rabuel, A. Jamali, C. Guéry, N. Recham

Laboratoire de Réactivité et de Chimie des Solides LRCS

CNRS UMR 7314

Université de Picardie Jules Verne

80039 Amiens, France

E-mail: nadir.recham@u-picardie.fr

T. Ouaneche, L. Stievano, F. Rabuel, C. Guéry, L. Monconduit,

M. T. Sougrati, N. Recham

Réseau sur le Stockage Electrochimique de l'Energie (RS2E)

FR CNRS 3459

80039 Amiens, France



Supporting information for this article is available on the WWW under https://doi.org/10.1002/batt.202400765

sustainable and cost-effective recycling, particularly for LFP batteries. Consequently, direct regeneration has emerged as a promising alternative, offering reduced energy consumption and enhanced economic viability.^[5,23–26]

Direct recycling of LFP is facilitated by the fact that its primary failure mechanism is the irreversible loss of lithium during the formation and growth of the solid electrolyte interphase (SEI) throughout cycling.^[20,27] Therefore, the key to successfully recovering spent LFP is to restore the original lithium inventory. Various studies have explored techniques for the direct recycling of LFP cathodes, including 1) high-energy ball milling followed by high-temperature solid-state reaction,^[22] and 2) hydrothermal reduction followed by annealing at high temperature.^[13,23,28] Recently, our group proposed a novel fast solvent-free lithiation process under ambient conditions, using LiI as both a reducing agent and a lithium source.^[29] This dry process has been successfully extended to other cathode materials, including LFMP, NMC, LMO, and LCO. However, the methods developed so far in the literature still face challenges related to high energy consumption and the extensive use of chemicals (solvents, reducing agents, lithium sources, etc.).

It is thus crucial to focus on more environmentally friendly regeneration processes. To address this challenge, we developed a green, cost-effective, and highly efficient regeneration process based on aqueous solution under ambient conditions, eliminating the need for heat or pressure. The main challenge with this process lies in managing the stability of LFP and FP in an aqueous medium. This issue is addressed by optimizing pH conditions and employing ascorbic acid (vitamin C), a highly effective reducing agent. Ascorbic acid is a well-known water-soluble antioxidant that predominantly exhibits pro-oxidant activity by reducing Fe^{3+} to Fe^{2+} .^[30] It has been largely used in chemical synthesis, notably by Whittingham et al.^[31] for the synthesis of olivine LFP via a hydrothermal process.^[32,33]

The regeneration process presented here occurs via an insertion lithiation in water at room temperature with stoichiometric quantities of reactants; it was optimized at the laboratory scale and subsequently upscaled, leading to the successful fabrication of new 18650 cells using 100% of regenerated LFP. These cells exhibited excellent performance comparable to 18650 cells containing 100% of pristine LFP.

2. Results and Discussion

The new regeneration method was first tested on chemically delithiated FP. Figure 1 shows the X-ray diffraction (XRD) patterns of both chemically delithiated olivine FP and the relithiated powders. The relithiation used the new process based on the green and cost-effective ascorbic acid as a reducing agent in combination with four lithium sources and in different ratios (cf., Table 1). The reaction is complete for all the experiments, with the total disappearance of the diffraction Bragg peaks of FP and the formation of pure olivine-type LFP. These results show that the $\text{Fe}^{II}\text{PO}_4$ reduction reaction accompanied by lithium insertion to obtain $\text{LiFe}^{II}\text{PO}_4$ is successful, with a rapid reaction kinetics (less than 10 min) at ambient air conditions and atmospheric pressure.

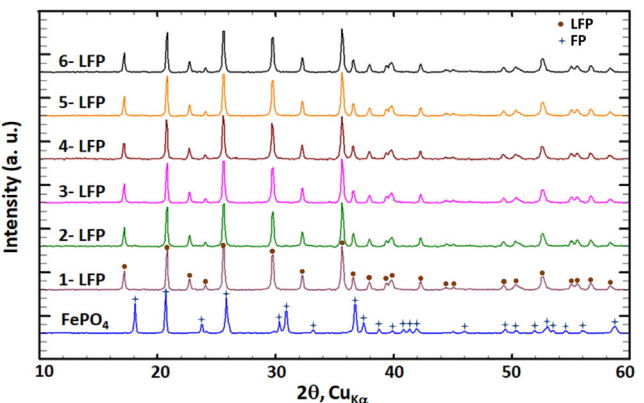


Figure 1. XRD patterns of the FePO_4 and the relithiated LiFePO_4 using ascorbic acid and five different lithium sources starting with: 1. lithium acetate ($\text{LiC}_2\text{H}_3\text{O}_2\cdot 2\text{H}_2\text{O}$), 2. lithium hydroxide ($\text{LiOH}\cdot \text{H}_2\text{O}$), 3. 2* lithium hydroxide ($\text{LiOH}\cdot \text{H}_2\text{O}$), 4. lithium carbonate (Li_2CO_3), 5. lithium sulfate (Li_2SO_4), and 6. 0.5* ascorbic acid with lithium hydroxide ($\text{LiOH}\cdot \text{H}_2\text{O}$), corresponding to the processes detailed in Table 1.

Table 1. Details for FP relithiation processes calculations containing the molar ratio of each experiment.

Process	Lithium source	Li mass [mg]	Li/red [mol]	FP/Li/red [mol]	pH
1	$\text{LiC}_2\text{H}_3\text{O}_2\cdot 2\text{H}_2\text{O}$ (Sigma-Aldrich; 98%)	≈136	1/1	1/1/1	3
2	$\text{LiOH}\cdot \text{H}_2\text{O}$ (Sigma-Aldrich; 99.9%)	≈56	1/1	1/1/1	6
3	$\text{LiOH}\cdot \text{H}_2\text{O}$	≈112	2/1	1/2/1	8
4	Li_2CO_3 (Sigma-Aldrich; 98%)	≈50	1/1	1/1/1	6
5	Li_2SO_4 (Sigma-Aldrich; 98.5%)	≈73	1/1	1/1/1	6
6	$\text{LiOH}\cdot \text{H}_2\text{O}$	≈56	2/1	2/2/1	6

These results confirm that FP can be efficiently relithiated using ascorbic acid in aqueous medium. The large choice of efficient lithium sources is beneficial for the global process price especially on the large scale.

Additionally, the results of process 6 (Table 1, Figure 1) show that one mole of ascorbic acid, which can offer two electrons according to Scheme S1, Supporting Information, can be efficiently used to regenerate (reduce) two moles of FP, which is important economically.^[30] Finally, some other reducing agents belonging to the ascorbic acid family can be used to achieve this lithiation reaction, such as sodium ascorbate. Figure S1, Supporting Information, shows the XRD pattern of delithiated FP and the obtained LFP powder after relithiation using sodium ascorbate as the reducing agent and lithium acetate dihydrate as the lithium source. It shows the complete disappearance of FP in favor of the pure olivine LFP, confirming the possibility of using other reducing agents of the ascorbic acid family under the same operating conditions.

Interestingly, these results show that FP lithiation to LFP can be carried out in a large pH domain (3–8), which is surprising since in the literature, LFP synthesis is always carried out in neutral^[34] or slightly basic media^[35] because of its stability and

solubility. This led us to study more precisely the FP and LFP stability in the acidic solution domain ($\text{pH} \approx 3$). For this, a study was carried out using a solution of HCl at $\text{pH} \approx 3$ to understand the LFP and FP behavior over time in this acidic lithiation domain.

Figure 2a,b shows the XRD patterns of pristine LFP and the obtained powders after remaining in a hydrochloric acid solution ($\text{pH} \approx 3$), for periods ranging from 30 min to 48 h in air and/or argon atmosphere. XRD shows the presence of LFP, and the appearance of FP after only 30 min to 1 h both in air and under argon atmosphere. This indicates the surprising partial oxidation of LFP to FP. This oxidation mechanism may be described in three steps: 1) the partial solubilization of LFP to generate Fe^{2+} in solution, in good agreement with the literature,^[33] 2) the oxidation of soluble Fe^{2+} by dissolved O_2 to form soluble Fe^{3+} , and 3) the oxidation of LFP to olivine FP with aqueous Fe^{3+} , which is reduced back to aqueous Fe^{2+} .

In the case of FP, **Figure 2c** shows the XRD patterns of both pristine olivine FP and the same powder after 48 h in HCl solution, showing in both the presence of pure FP. Moreover, the recovered amount was very close to that introduced at the beginning of the experiment, indicating that FP is stable and does not evolve in hydrochloric acid, even though a partial amorphization, undetectable by XRD, cannot be excluded. Electrochemical tests (Figure S2, Supporting Information), nevertheless, show the pure signature of olivine FP, confirming the stability of FP under these

conditions. In summary, these results show that, in hydrochloric acid solution, FP is stable and LFP partially oxidizes to form FP.

Impressively, even though no evolution of LFP during the lithiation process in ascorbic acid solution at $\text{pH} \approx 3$ was observed, the stability of both LFP and FP was verified in the acidic lithiation medium for longer periods of time. First, the stability of pristine LFP over time was checked using a solution of ascorbic acid at $\text{pH} \approx 3$ in air. **Figure 3a** shows the XRD patterns of LFP in the pristine state and after immersion in ascorbic acid solution for various periods of time ranging from 10 min to 48 h. The XRD patterns of these materials show that olivine LFP is stable over time in this acidic medium, as it is the only detected phase. Even if a very small amount of LFP were dissolved, no FP formation could be observed, probably thanks to the reducing power of ascorbic acid which keeps the dissolved Fe^{2+} in the reduced state. This stability was confirmed by the galvanostatic tests shown in **Figure 3b**, which show the typical electrochemical signature of LFP versus Li, and the absence of the FP reduction plateau or of the amorphous FP signature during the first discharge.

On the other hand, the same study carried out starting from olivine FP (cf., **Figure 3c**) shows the gradual disappearance of the XRD pattern of FP after 5 h, and its total suppression after 1 week, indicating the gradual amorphization of FP and its completion after 1 week. This means that ascorbic acid, known for its complexation and reduction properties, most probably reduces and

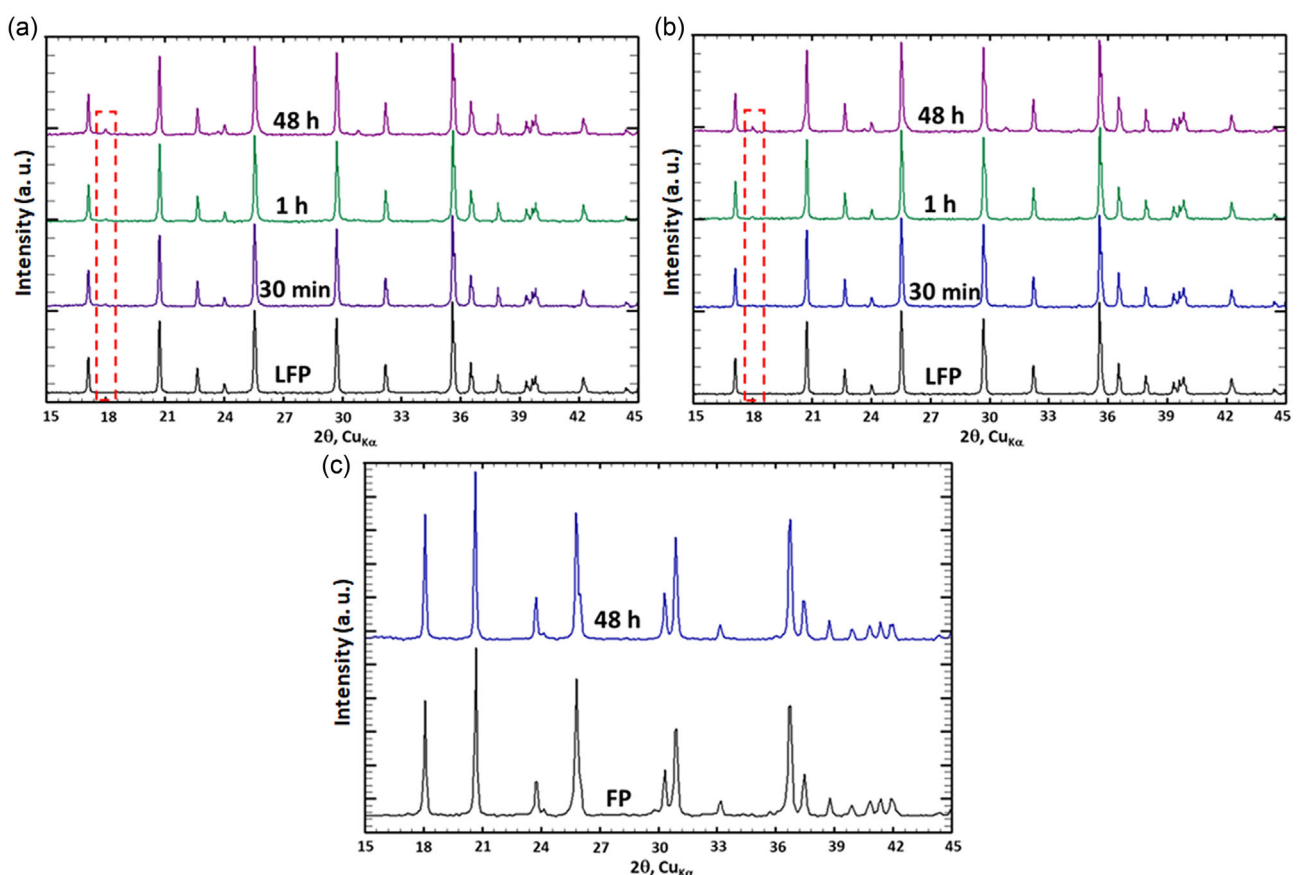


Figure 2. Stability study: XRD patterns of pristine LFP and the obtained powders after 30 min, 1 h, and 48 h in HCl solution ($\text{pH} \approx 3$) a) in air and b) under argon atmosphere, and c) XRD patterns of olivine FP and the obtained FP powder after 48 h in HCl solution in air.

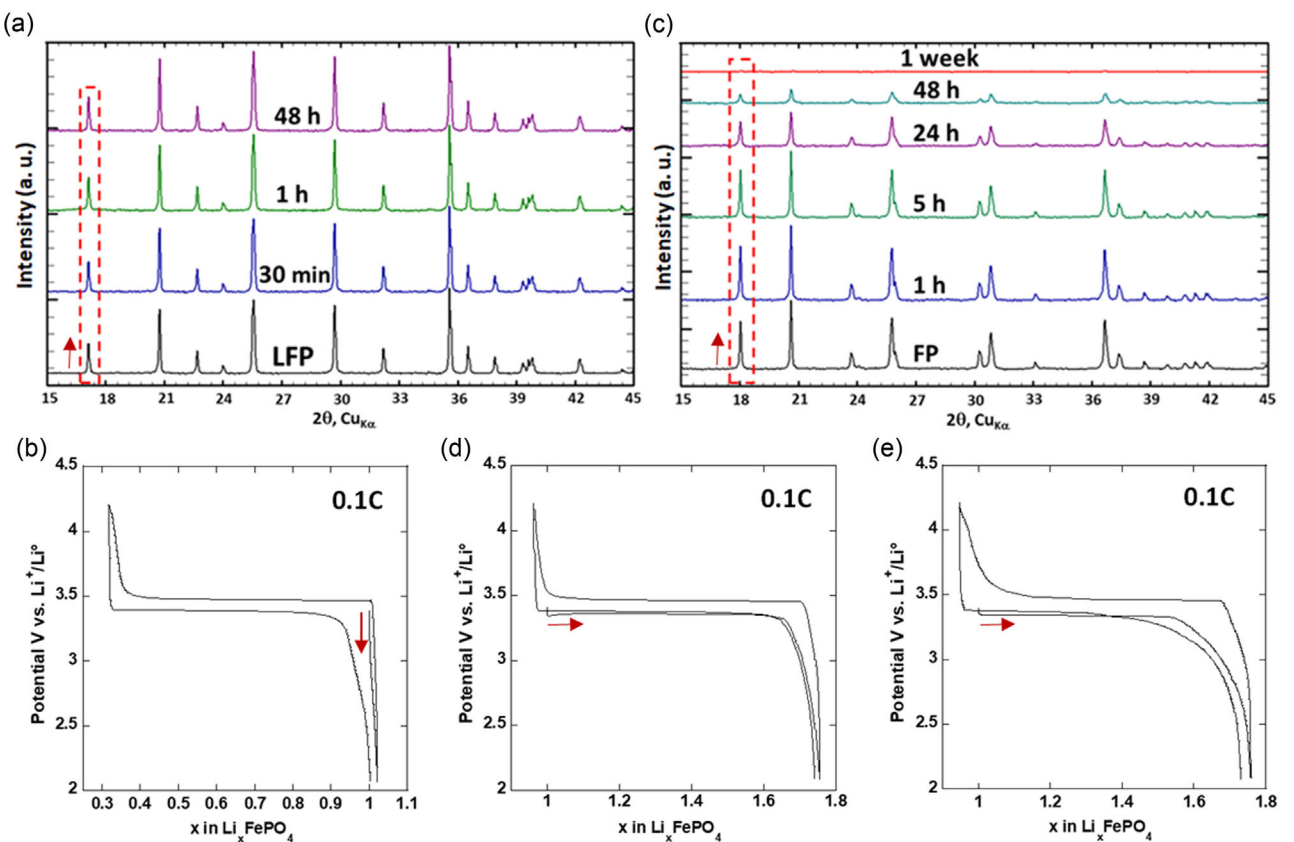


Figure 3. a) XRD patterns of pristine LFP and the obtained powders after 30 min, 1 h, and 48 h in the lithiation domain of ascorbic acid solution ($\text{pH} \approx 3$) in air and b) the electrochemical performance in galvanostatic mode of the obtained LFP powder (after 48 h in the solution) versus Li metal at 0.1C, c) XRD patterns of olivine FP and the obtained powders after 1, 5, 24, 48 h and 1 week in ascorbic acid solution in air, and the electrochemical performance of the obtained FP powders after d) 1 h and e) 5 h in the solution versus Li metal at 0.1C.

solubilizes FP producing solvated Fe^{2+} species. Since the reaction occurs in air, dissolved O_2 may oxidize solvated Fe^{2+} to Fe^{3+} , leading to the precipitation of amorphous $\text{FP}\cdot\text{xH}_2\text{O}$.^[36]

These results are confirmed by electrochemistry, as olivine FP after 1 h in the ascorbic acid solution produces a perfectly regular and stable olivine electrochemical signature (Figure 3d), with a single plateau both in discharge and in charge, and an average potential of 3.44 V versus Li^+/Li^0 . For FP after 5 h in the ascorbic acid solution, however, a first plateau is observed during the first discharge (Figure 3e), corresponding to the reaction of about 0.55 Li^+ , followed by a second process with an increasingly steep slope (the potential decreases with the composition) of about 0.2 Li^+ . These signals are reversibly observed also during the charge. While the first plateau corresponds to the (de)insertion of Li^+ in the olivine structure, the second phenomenon can be attributed to the reaction of amorphous hydrated FP species, in line with the XRD results.

Summarizing, an acidic pH does not directly produce FP amorphization, which rather depends on the reducing/complexing power of ascorbic acid (and possibly of the species produced by its oxidation in air) if a lithium source is absent in the solution. Even if FP is unstable in ascorbic acid solutions, its amorphization is relatively slow and can be avoided thanks to the rapid kinetics of the relithiation which occurs in less than 10 min.

This study of the relative stability of LFP and FP in these solutions allows optimizing the lithiation conditions while avoiding parasite decomposition reactions and is particularly important in view of the scaling-up of this lithiation process to treat large amounts of spent LFP. Following these results, the following options for the lithiation of FP to LFP should be considered for an industrial application: 1) use of LiOH or Li_2CO_3 in order to get an appropriate pH and avoid LFP solubilization, and 2) use of Ar/N_2 controlled atmosphere, or the use of ascorbic acid in excess in air to protect lithiated LFP from oxidation by dissolved O_2 .

Based on these very promising results, the same lithiation process was applied to a larger amount of EOL LFP cathode powder (S-LFP) recovered from spent LFP/graphite 26650 cells. Figure 4 shows the S-LFP electrode pieces before and after the single-step treatment with TEP, which is able to separate of LFP from the aluminum current collector via the partial solubilization of the PVDF polymer binder.^[37] The shiny glare of the Al current collector after the treatment confirms its effective separation of coated LFP with no visible surface corrosion. This separation process allowed the easy recovery of 140 g of LFP powder mixture from the spent 26650 cells, which was thoroughly ground in a mortar to obtain a homogeneous powder and used for the lithiation process.

The refined XRD pattern of the S-LFP powder, shown in Figure 5a, confirms the presence of both olivine (triphylite) LFP



Figure 4. Photos showing the spent LFP cathode, recovered powder and aluminum foils which correspond to the AM/AI separation step using triethyl phosphate (TEP) solvent.

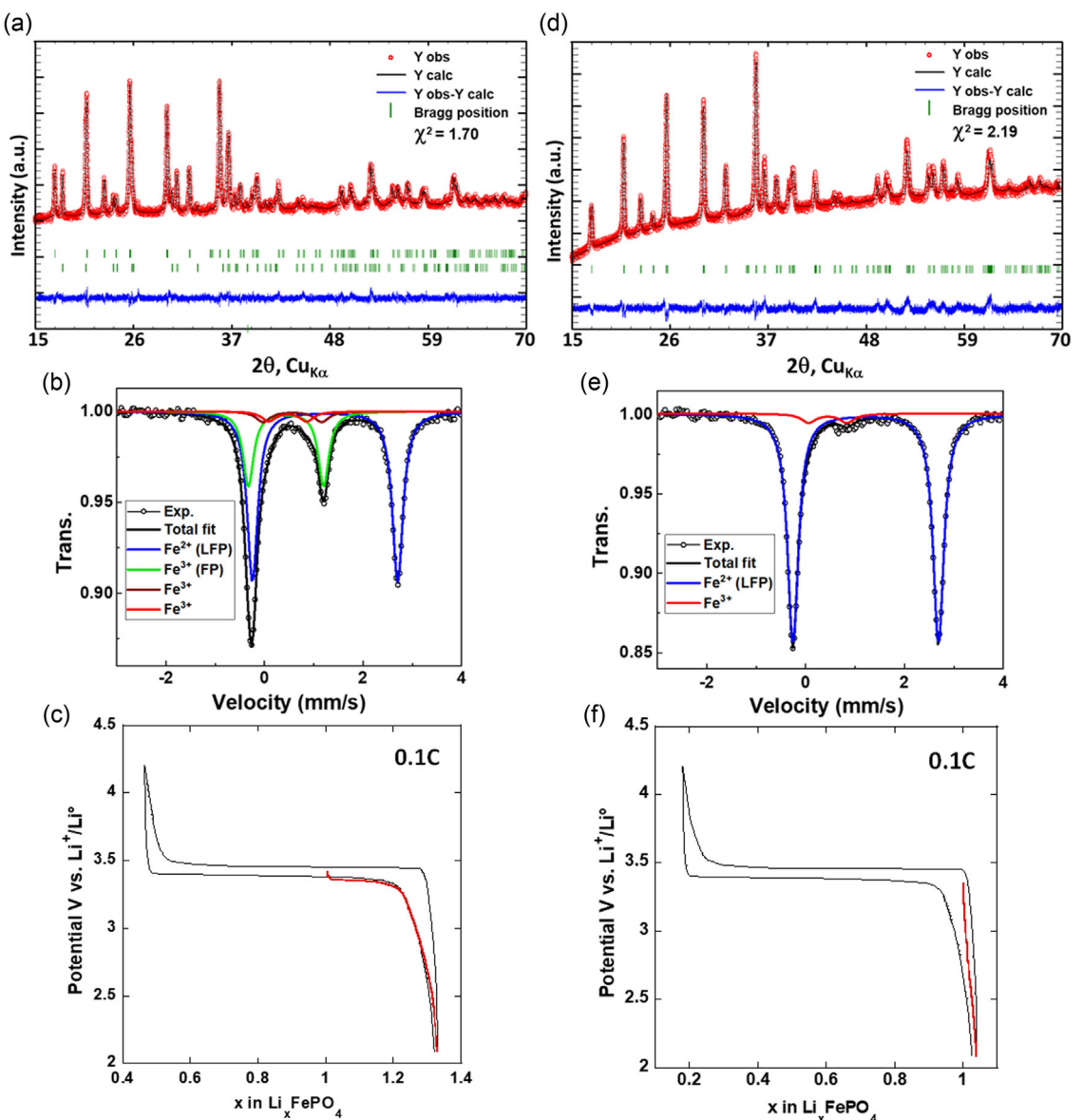


Figure 5. Spent LFP cathode powder mixture characterization by a) Rietveld refinement of the XRD pattern, b) Mössbauer spectroscopy, and c) discharge-charge galvanostatic curves at 0.1C (1 electron in 10 h) of the spent LFP cathode mixture as positive electrode versus Li^+/Li^0 , and lithiated LFP cathode powder mixture characterization by d) Rietveld refinement of the XRD pattern, e) Mössbauer spectroscopy, and f) discharge-charge galvanostatic curves at 0.1C of the lithiated LFP cathode mixture as positive electrode versus Li^+/Li^0 .

(space group Pnma, $a = 10.312(1)$ Å, $b = 5.999(1)$ Å, $c = 4.696(1)$ Å), and olivine (heterosite) FP (space group Pnma, $a = 9.822(1)$ Å, $b = 5.791(1)$ Å, $c = 4.783(1)$ Å). This result is confirmed by

Mössbauer spectroscopy (Figure 5b), which shows the presence of ≈62% LFP and ≈27% FP (Table 2), together with minor amounts of amorphous impurities corresponding to ≈10%

Table 2. Mössbauer hyperfine parameters of: S-LFP powder and relithiated S-LFP powder. δ , Δ , Γ , and area correspond to the isomer shift, the quadrupole splitting, the linewidth, and the relative resonance area, respectively.

Samples	δ , [mm s ⁻¹]	Δ , [mm s ⁻¹]	Γ , [mm s ⁻¹]	Area, [%]	Attribution
S-LFP powder (Figure 5b)	1.22	2.95	0.26	62.4	LFP (Fe^{2+})
	0.43	1.53	0.26	27.4	FP (Fe^{3+})
	0.56	1.19	0.35	5.3	(Fe^{3+})
	0.47	0.77	0.35	4.9	(Fe^{3+})
Lithiated S-LFP (Figure 5e)	1.22	2.94	0.26	95	LFP (Fe^{2+})
	0.45	0.77	0.35	5	(Fe^{3+})

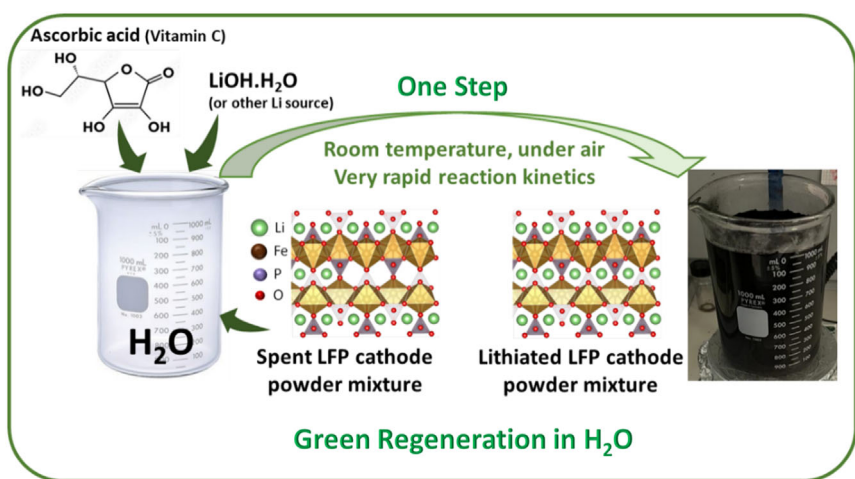
(atomic ratio) of the total resonance area. These two other Fe^{3+} environments are relatively common and are usually attributed to Fe_2P impurities formed during the synthesis of pristine LFP at high temperature under reductive environment.^[38] In this case, the lithium loss is directly related to the relative amount of the FP in the S-LFP cathode.

The galvanostatic cycling curve of the S-LFP powder in half-cell versus lithium metal at 0.1C (Figure 5c) shows the typical electrochemical signature of LFP, with a stable reversible capacity of $\approx 150 \text{ mAh g}^{-1}$ after the first charge. About $\approx 0.3 \text{ Li}^+$ are inserted per mole of LFP in the first discharge, corresponding to the reduction of the residual fraction of FP (about 30%) in S-LFP. This observation is in good agreement with both XRD and Mössbauer spectroscopy, confirming that about 30% of the lithium inventory is missing in the pristine S-LFP cathode even though the batteries were discharged to 0.5 V.

The S-LFP powder was then treated using the previously described lithiation process in aqueous solution (Scheme 1). The refined XRD pattern of the relithiated powder (Figure 5d) exhibits only the reflections of pure olivine LFP with lattice parameters $a = 10.323(3) \text{ \AA}$, $b = 6.003(4) \text{ \AA}$, and $c = 4.692(4) \text{ \AA}$, virtually identical to the literature values,^[39] indicating the complete lithiation of LFP cathode. This result is confirmed by Mössbauer spectroscopy (Figure 5e), which shows the total disappearance of Fe^{3+} (FP) and the presence of 95% Fe^{2+} (LFP), the remainder 5% Fe^{3+} being represented by amorphous impurities (cf., Table 2)

already contained in the pristine material. The electrochemical performance of the relithiated LFP powder, evaluated by galvanostatic cycling at 0.1C in half-cell configuration versus Li metal (Figure 5f), shows the typical biphasic process of LFP at an average potential of 3.44 V. In the first discharge, no additional capacity is registered, confirming the full relithiation of the material. A reversible capacity of $\approx 150 \text{ mAh g}^{-1}$, not so far from the expected theoretic one, is obtained during the following cycles.

In order to investigate the state of the carbon coating on the LFP particles after regeneration, a Transmission electron microscopy (TEM) study was carried out. The low-magnification and the high-resolution TEM (HRTEM) images of spent and regenerated S-LFP are shown in Figure 6. The S-LFP particles (Figure 6a) are irregularly shaped with an average size of nearly 200 nm. The chemically lithiated S-LFP shows similar particle morphology and size, as evidenced by the low-magnification images (Figure 6c,d). The carbon coating of the S-LFP particles is clearly visible by HRTEM (Figure 6b,e). Since chemical relithiation does not involve any high-temperature treatment, the carbon coating layer is preserved after the treatment, as confirmed by HRTEM (cf., Figure 6e). The thickness of the carbon coating layer is estimated at 3 nm, close to the literature value,^[40] and does not vary after chemical relithiation. In summary, these results confirm that the proposed room-temperature relithiation process not only produces no morphological modification in the LFP particles but also preserves their surface carbon coating.



Scheme 1. Simplified process diagram of spent LFP cathode lithiation.

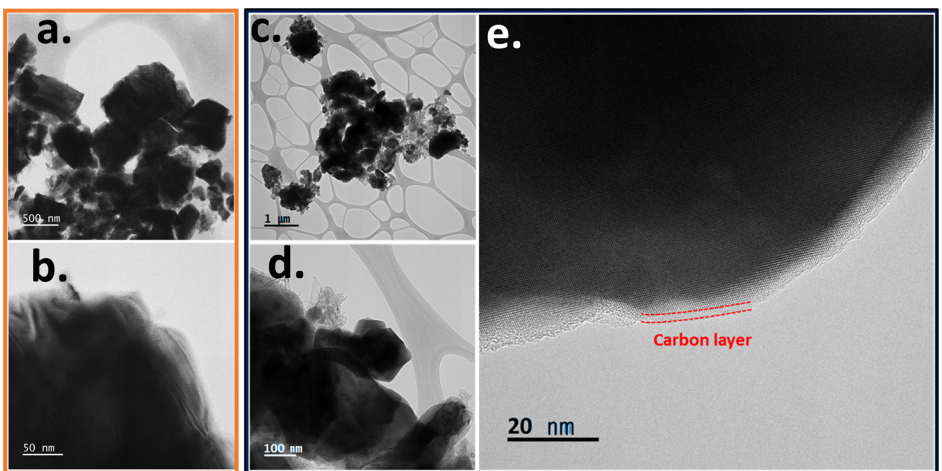


Figure 6. Low-magnification and high-resolution TEM images of a,b) spent LFP cathode and c–e) regenerated LFP cathode.

Before testing the electrochemical performance of regenerated S-LFP in 18650 full cells versus graphite, its cyclability was studied in half-cell configuration versus Li metal at increasing current rates from 0.1C to 3C (Figure S4, Supporting Information). A discharge capacity of 165 mAh g^{-1} is obtained at 0.1C, which decreases to 160 mAh g^{-1} at 0.2C and to 140 mAh g^{-1} at 1C. At 3C, the discharge capacity drops rapidly from 80 to 35 mAh g^{-1} . In spite of this rapid capacity decrease, these results are promising since the material exhibits around 85% of its initial capacity at 1C and recovers the total initial capacity when cycled back at 0.1C.

The electrochemical performance of the fully relithiated S-LFP (R-LFP) was finally tested in LFP/graphite 18650 cells and compared to similar cells produced with pristine LFP (P-LFP) and with a mixture of pristine LFP containing 15 wt% regenerated LFP (r-LFP).

Figure 7a shows the galvanostatic curves of the first cycle at 0.05C and the second and tenth cycles at 0.2C as well as the capacity retention for the first ten cycles of R-LFP full cell. The cell exhibits the typical electrochemical profile of a LFP/graphite battery with an average potential of 3.2 V. The first charge and discharge capacities at 0.05C are 1.29 and 1.07 Ah, respectively. This irreversible capacity loss could correspond to the formation of the SEI, which continues along the first five cycles at 0.2C. From the following cycle, the reversible capacity remains stable at 1.05 Ah. A similar electrochemical behavior is shown by the r-LFP and P-LFP cells, shown in Figure 7b and Figure S3, Supporting Information, with respective first charge capacities of 1.15 and 1.12 Ah and first discharge capacities of 0.96 and 0.94 Ah at 0.05C. After the first five cycles and the full formation of the SEI, the reversible capacity stabilizes at 0.9 Ah for both cells. This slight difference in capacity compared with R-LFP cell can be explained by the difference in the mass of active material in the cells (cf., Table 4).

The long cycling performance of the three cells along 100 cycles at 0.5C is gathered in Figure 8a. Discharge capacities of 0.95–0.93, 0.88–0.85, and 0.87–0.84 Ah are recorded for R-LFP, r-LFP, and P-LFP cells, respectively. In addition, the inset in Figure 9a shows their excellent coulombic efficiency exceeding

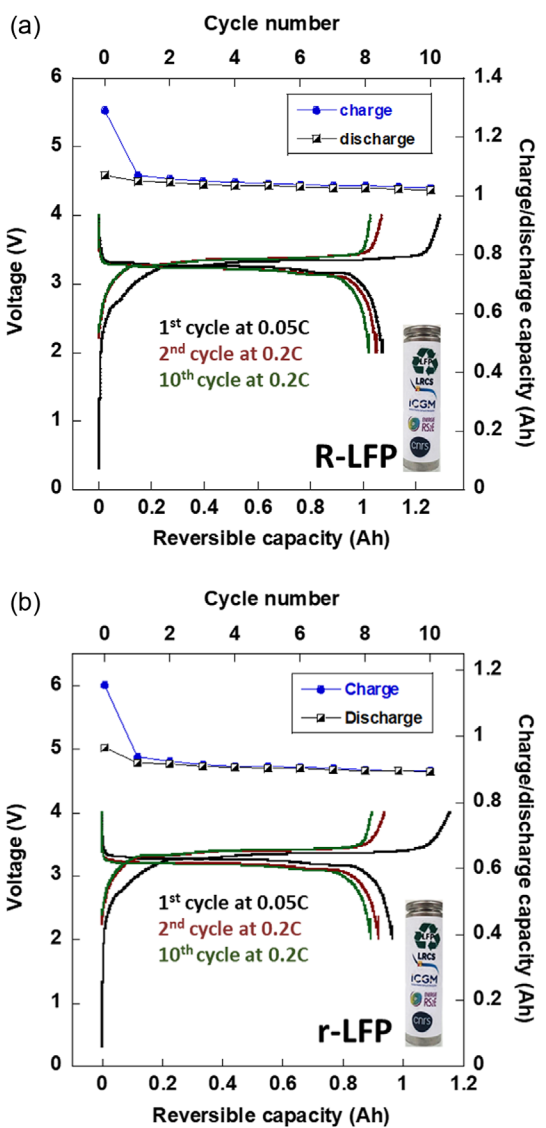


Figure 7. Electrochemical performance during SEI formation shown by: charge/discharge galvanostatic curves for the first cycle at 0.05C with the second and tenth cycles at 0.2C, and the reversible capacity recorded for the first ten cycles, corresponding to: a) R-LFP and b) r-LFP 18650 cells.

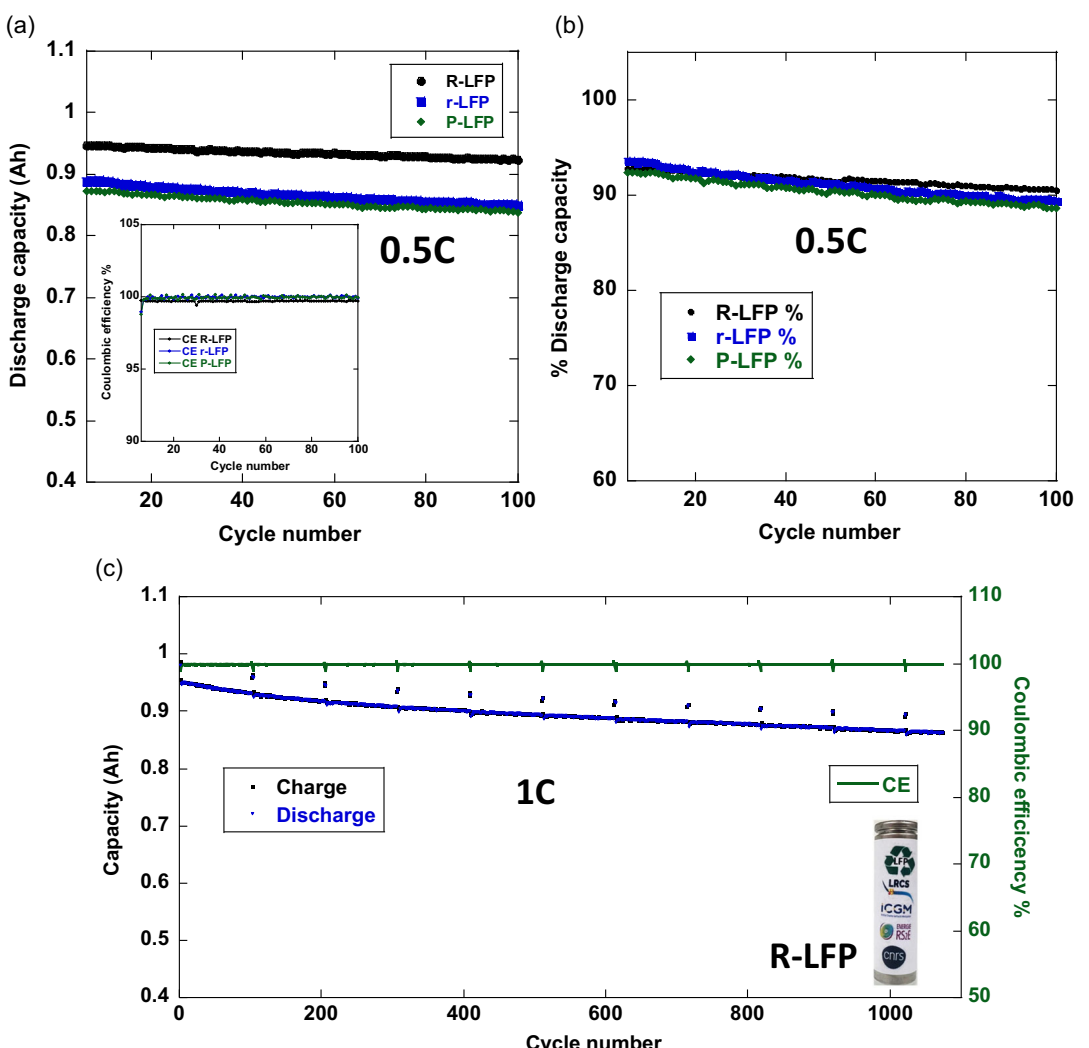


Figure 8. a) Electrochemical cycling performance in discharge of R-LFP, r-LFP, and P-LFP full (LFP/graphite) 18650 cells, at 0.5C for 100 cycles, with their inserted coulombic efficiencies. b) % discharge capacity of R-LFP, r-, and P-LFP at 0.5C, and c) charge/discharge capacity of R-LFP at 1C rate for more than 1000 cycles with its coulombic efficiency.

99%. All cells show a similar good capacity retention between 93% and 88% of the initial capacity during the 6th and the 100th cycles (Figure 8b).

The cycling of the R-LFP cell was prolonged at 1C rate for more than 1000 cycles (Figure 8c), exhibiting a capacity of 0.95 Ah and 0.87 Ah for the 1st and the 1000th cycles at 1C, respectively, and showing an excellent capacity retention of $\approx 92\%$. This cell also shows a remarkably good and stable coulombic efficiency exceeding 99%. These results show that the regenerated LFP presents the same electrochemical properties of the pristine material and confirm that it is possible to efficiently combine pristine LFP with a certain amount of recycled LFP (15% in our case for r-LFP) to produce new cells, in line with the European standards requiring the implementation of a minimum of 10% recycled lithium in new cells by 2035.^[15]

For further practical applications, the relationship plot between specific power (W kg^{-1}) and specific energy (Wh kg^{-1}) is imperative in the evaluation of electrode materials. This cycling process enables the measurement of battery

performance under constant power cycling and correlates the power versus energy performance using normalized values.^[41] The Ragone plot for R-LFP and P-LFP cells in Figure 9a shows that the materials retain their energy storage ability, with R-LFP providing a slightly higher specific energy ($\approx 96 \text{ Wh kg}^{-1}$) than P-LFP ($\approx 87 \text{ Wh kg}^{-1}$). It is worth noting that the pristine and spent LFP are not from the same supplier. This test confirms that the applied recycling process has no negative effects and that the recycled LFP can be used for the same applications as commercial LFP, once again confirming the efficiency of the developed direct lithiation process.

In real life, a battery is used under various conditions and is submitted to variable charge/discharge processes at different current rates. For this reason, the cycling performance of the R-LFP cell was evaluated at different C rates. As shown in Figure 9b, R-LFP exhibits a discharge capacity of 1.05 Ah at 0.1C in the first cycle and 1.02 Ah for the ten next cycles at 0.2C. A stable discharge capacity of 1 Ah is obtained at 0.5C followed by 0.99 Ah at 1C and 0.97 Ah at 2C. The discharge capacity slightly

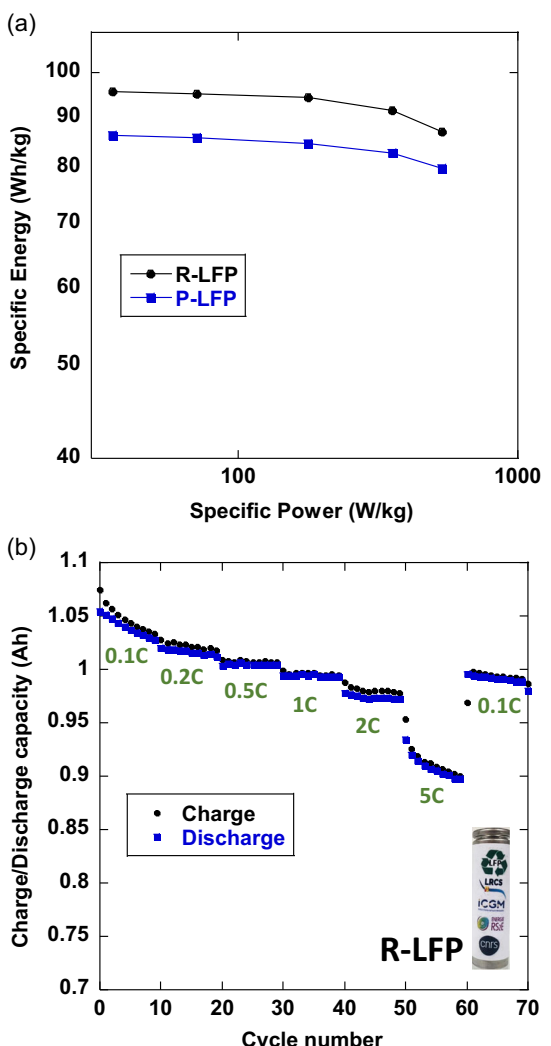


Figure 9. a) Ragone plots of energy density versus power density of R-LFP and P-LFP 18650 full cells and b) R-LFP rate performance at different current rates (0.1, 0.2, 0.5, 1, 2, 5, and 0.1C) for 70 cycles.

decreases to 0.9 Ah at 5C, which represents 86% of the initial discharge capacity of the cell. An increase in capacity is then observed over the last ten cycles at 0.1C, reaching 1 Ah. These results confirm the very good capacity retention of this cell containing recycled LFP, as well as its remarkable resilience to variations in cycling rate. Finally, this study demonstrates that the regenerated LFP cathode is suitable for high power applications.

3. Conclusion

A very promising one-step lithiation process using a green and non-toxic reducing agent, ascorbic acid (vitamin C), with a lithium source in aqueous solution allows the very efficient relithiation of spent LFP recovered from EOL LIBs. Such a process offers significant advantages including application at room temperature in air, fast reaction kinetics, use of water as the solvent, no need of heating, and widespread availability of the used reagents. The exceptional efficiency of this method for the complete relithiation

of spent LFP is confirmed by various characterization techniques including XRD, Mössbauer spectroscopy, electrochemical analyses, and TEM.

A detailed study of LFP and FP stability in the lithiation medium is crucial for process scale-up. The developed process was effectively applied on an intermediary scale, leading to the reformulation of fully recycled LFP electrodes used in the fabrication of recycled LFP/graphite 18650 pilot cells with a capacity of 1.05 Ah. These cells exhibit excellent electrochemical performance compared to a pristine LFP/graphite 18650 cell. This achievement undoubtedly paves the way for industrial applications of this method while contributing to the sustainable management of LIBs and the advancing the transition to a circular economy.

4. Experimental Section

Lithiation Process

Chemically delithiated FePO_4 (FP) powder was obtained by chemical delithiation of pristine commercial LFP (Targray) using iron(III) nitrate nonahydrate $\text{Fe}(\text{NO}_3)_3 \cdot 9\text{H}_2\text{O}$ ($\geq 98\%$) in aqueous solution for 12 h. For each relithiation experiment, ≈ 234 mg of ascorbic acid $\text{C}_6\text{H}_8\text{O}_6$ (Sigma-Aldrich; 99%) was added to a water suspension of FP (200 mg) as a reducing agent, together with either $\text{LiC}_2\text{H}_3\text{O}_2 \cdot 2\text{H}_2\text{O}$, $\text{LiOH} \cdot \text{H}_2\text{O}$, Li_2CO_3 , or Li_2SO_4 as the lithium source (cf., Table 1). The suspensions were stirred for 10 min at room temperature in ambient air before separating the solid fraction by centrifugation, washing it with ethanol and drying it at 60°C under primary vacuum for 1 h.

LFP/FP Stability in Acidic Solution

The stability of LFP and FP in ascorbic acid solution was investigated by adding 200 mg of LFP and 224 mg of ascorbic acid in ≈ 30 mL H_2O in air ($\text{pH} \approx 3$). The study was carried out as a function of time, starting from 10 min to 1 week under weak stirring. At the end of the experiment, the powders were recovered by centrifugation, washed with ethanol, and dried at 60°C under primary vacuum for 1 h. The same process was carried out using 200 mg of olivine FP with 234 mg of ascorbic acid in ≈ 30 mL H_2O in air.

The stability of LFP and FP was also investigated in a 10^{-3} mol L^{-1} hydrochloric acid solution ($\text{pH} \approx 3$), which was prepared by adequately diluting a commercial solution of HCl 37% (VWR) in deionized water. In the case of LFP, 200 mg was used in around 30 mL of the HCl solution and stirred as a function of time, starting from 30 min to 48 h. The study was carried out both in air and under argon atmosphere. The same evaluation was carried out using 200 mg of FP powder in 30 mL of the HCl solution in air.

Scale-Up Process

With the aim of scaling it up, the developed lithiation process was applied to a large quantity of spent LFP cathodes. This was made using ten different aged 26650 LFP/graphite commercial cells at different stages of their life (20–80%). The cells were discharged to 0.5 V and opened in dry room atmosphere. After dismantling the battery, the negative and positive electrodes were separated, then the spent LFP cathodes were recovered, washed in dimethyl carbonate (DMC), and dried under primary vacuum at 90°C . In order to separate the spent electrode powder mixture LFP/C/PVDF from its aluminum current collector, triethyl phosphate TEP (Thermo Scientific, 99%),

commonly considered as a green solvent, was used.^[42] To do so, each recovered LFP electrode film was cut into around $2 \times 4\text{ cm}$ (8 cm^2) pieces which were introduced into $\approx 800\text{ mL}$ of TEP solvent under argon atmosphere and then heated at 100°C for 4 h. The cathode powder, completely removed from the current collector, was recovered by filtration, washed with ethanol, and dried under primary vacuum at 90°C . The dried material was ground in a mortar to obtain a homogeneous powder, which was then hand-sieved to $80\text{ }\mu\text{m}$. The sieved LFP electrode powder mixture (S-LFP) was used for the ensuing lithiation process after determining the relative amounts of LFP and FP by electrochemistry and Mössbauer spectroscopy.

The lithiation was carried out by solubilizing $\approx 46\text{ g}$ of ascorbic acid $\text{C}_6\text{H}_8\text{O}_6$ and $\approx 17\text{ g}$ of lithium hydroxide monohydrate $\text{LiOH}\cdot\text{H}_2\text{O}$, with a molar ratio of 1/1.5, in $\approx 800\text{ mL H}_2\text{O}$ in air ($\text{pH} \approx 7\text{--}8$). Under these conditions, the total molar ratio of FP/Ascorbic acid/Li is 1/1/1.5. The amount of reducing agent and lithium source were determined based on the FP content in the S-LFP cathode powder which corresponds to $\approx 28\%$. After a complete solubilization of both powders, 140 g of the S-LFP powder was added to the solution. The suspension was stirred for 1 h at room temperature in air, and then the solid was filtered and rinsed with ethanol. The obtained powder was dried under primary vacuum at 90°C .

Cylindrical 18650 LFP/Graphite Cells Formulation

The successfully lithiated LFP powder was used to reformulate new electrode films (see the details below) in order to build new cylindrical 18650 commercial-type cells with two different configurations: 1) completely recycled LFP cathode (R-LFP), 2) pristine LFP (Targray Canada) mixed with 15 wt% recycled LFP powder (r-LFP), and graphite as negative electrode. In addition, 18650 cells containing only pristine LFP cathodes were also made and used as references (P-LFP). The formulation steps were carried out in a prototyping dry room equipped with all the equipment needed to produce commercial 18650 cells (Scheme S2, Supporting Information). The following sections will detail the fabrication steps of the positive and negative electrodes.

Positive Double-Side Coated Electrode Slurry

The formulation of R-LFP electrodes was done by mixing overnight the active material with conductive carbon (C45) and polyvinylidene fluoride PVDF (Solef 5130) polymer as the binder, with a mass ratio of 95/3/2 for LFP cathode/C/PVDF, using a 3D shaker mixer Turbula (WAB). The mixed powder was then mixed with *N*-methyl-2-pyrrolidone NMP solvent (MSESUPPLIES) using a Dispermat (VMA-GETZMANN) high-shear mixer for 2 h in a water-bath cooled recipient at 25°C , with a dry mass/solvent ratio of 45/55. The slurry was coated onto a $16\text{ }\mu\text{m}$ thick aluminum foiling using a comma-coater prototype-grade machine (PDL250, People & Technology, Korea) fixing the coating speed at 0.3 m min^{-1} . The electrodes were dried in a built-in two-part oven at 70 and 80°C , corresponding with previously optimized temperatures for the LFP slurries in our pilot line.

The same formulation steps were followed for the second positive electrode configuration r-LFP (pristine LFP mixed with 15 wt% recycled LFP), with a mass ratio of 90/5/5 for LFP/C/PVDF. This same configuration was also used in order to formulate the P-LFP electrode used in the reference pristine LFP/graphite cells.

Negative Double-Side Coated Electrode Slurry

The formulation of negative graphite electrodes was done by mixing graphite GHDR 15-4 with C45 conductive carbon, carboxymethyl celulose binder CMC-700 K DS = 0.9, styrene butadiene elastomer SBR

Table 3. Details of electrodes formulation composition.

Electrode	Chemicals	Mass ratio	Supplier
R-LFP	LFP cathode	93	–
	C45	3	Imerys-France
	PVDF Solef 5130	2	Solvay
r-LFP	LFP cathode	90	–
	C45	5	Imerys-France
	PVDF (Solef 5130)	5	Solvay
P-LFP	LFP	90	Targray Canada
	C45	5	Imerys-France
	PVDF (Solef 5130)	5	Solvay
Graphite	graphite GHDR 15-4	93.2	Imerys-France
	C45	3	Imerys-France
	CMC-700 K DS = 0.9	2.5	Acros
	SBR BM-451B	1	Zeon
	Triton X-100	0.3	Sigma Aldrich

BM-451B and Triton X-100 polymer with global mass ratios of 93.2/3/2.5/1/0.3. H_2O was then added to the mixture and mixed overnight in a Dispermat with a dry mass/solvent ratio of 42/58. The slurry was cast onto a copper foil ($11\text{ }\mu\text{m}$ thickness) using a comma-coater prototype-grade equipment. The electrodes were dried in a built-in two-part oven at 70 and 80°C . The details of each electrode slurry formulation are presented in Table 3.

Cylindrical 18650 LFP/Graphite Cells: Electrodes Calendering

After drying process, the electrodes were calendered with a prototype-grade lap press calender (BPN250, People & Technology, Korea). The latter consists of a two-roll compactor of 25 cm in diameter. The main characteristics, mass loading, porosity, and thickness, of the formulated electrodes R-LFP, r-LFP, P-LFP, and graphite are reported in Table 4.

It is worth noting that graphite was slightly used in excess to achieve the full capacity of the LFP. For this, the cell balancing in terms of the mass capacity ratio of graphite/LFP is: 1.23, 1.3, and 1.34 for R-LFP, r-LFP, and P-LFP, respectively.

Cylindrical 18650 LFP/Graphite Cells Assembly

Once the positive and negative electrodes were formulated, calendered, and cut according to 18650 cell format, the winding step was completed in prototyping room using a PE separator of $16\text{ }\mu\text{m}$ thickness. The cells were then dried under primary vacuum at 90°C for 3 days. 6.5 g of commercial LP30 electrolyte (DoDo Chem) containing 1 M lithium hexafluorophosphate LiPF_6 dissolved in a solution of ethylene carbonate and DMC with 1:1 weight ratio

Table 4. Main characteristics of the dried electrodes R-LFP, r-LFP, P-LFP, and graphite.

Electrode	Mass loading [mg cm^{-2}]	Porosity [%]	Thickness [μm]
R-LFP	16.21	43.8	196
r-LFP	15.30	50.3	208
P-LFP	14.80	50	197
Graphite	8.30	35	136

was added to each cell. The cells were then sealed and left resting overnight to ensure the appropriate impregnation of electrodes and separator with the electrolyte.

Physicochemical Characterization

XRD measurements were carried out using a Bruker D8 Advance powder diffractometer equipped with the Cu K α radiation ($\lambda_{K\alpha 1} = 154,056 \text{ \AA}$ and $\lambda_{K\alpha 2} = 154,439 \text{ \AA}$) and a Lynkeye detector operating at 40 kV and 40 mA. XRD patterns were collected between 15° and 45° (2 Θ) for 30 min with a step of 0.0368 for routine measurements. Additional high-resolution XRD patterns were collected between 15° and 70° (2 Θ) for 10 h with a step of 0.02 and fitted using full Rietveld refinement as implemented in the FULLPROF software.

Transmission ^{57}Fe Mössbauer spectra were recorded at room temperature in the constant acceleration mode with a $^{57}\text{Co}:\text{Rh}$ source. The Mössbauer absorbers were prepared with 20–50 mg cm $^{-2}$ of cathode materials. The isomer shifts are given with respect to α -Fe metal at room temperature. The velocity scale was set between $\pm 4 \text{ mm s}^{-1}$, and the acquisition time between 24 and 36 h to obtain a reasonably good signal-to-noise ratio.

In order to check the state of the carbon coating on the LFP particles after regeneration, TEM was carried out using a FEI Tecnai F20-STWIN microscope, equipped with a OneView camera (Gatan Inc., Pleasanton, CA, USA), and operating at an accelerating voltage of 200 kV. Samples were prepared by suspending the powder in ethanol and sonication for 5 min. A 10 μL droplet was then placed onto a 200-mesh copper TEM grid, dried, and stored for observation.

Electrochemical Characterization

The electrochemical properties of LFP cathode powder mixture at different stages of the regeneration process were tested in half-cell configuration versus Li metal in galvanostatic mode at the rate of 0.1C (corresponding to the reaction of 1 lithium in 10 h), between 2.1 and 4.2 V. For these tests, Swagelok-type cells were assembled in an argon-filled glove box using around 10 mg cm $^{-2}$ of electrode composite powder containing the LFP cathode powder hand-mixed with 10 wt% of conductive carbon C45. The two electrodes (LFP vs Li metal) were separated by one sheet of glass fiber disk (Whatman GF/D) soaked with commercial LP30 electrolyte.

The electrochemical performance of the relithiated LFP after cathode reformulation was conducted using electrode disks of 13 mm of diameter and a mass loading of 16 mg cm $^{-2}$, which were punched on their aluminum current collector and directly used in 2032 Coin cells assembled in dry room atmosphere ($\text{H}_2\text{O} < 15 \text{ ppm}$). The cells were prepared using the same configuration mentioned above and cycled at different current rates starting with 0.1, 0.2C, 1C, 3C, and 0.1C, where ten cycles were registered for each current rate.

Finally, the LFP/graphite 18650 assembled cells were cycled at room temperature between 2 and 4 V. They were first cycled in galvanostatic mode at a current rate of 0.05C, followed by ten cycles at 0.2C in order to allow the formation of the SEI. After this, different cycling programs were used in order to study the electrochemical performance: 100 cycles at 0.5C rate for each type cell, and more than 1000 cycles at 1C rate for the totally recycled R-LFP cell with one cycle at 0.1C after every 100 cycles. A rate capability (successively at 0.1, 0.2, 0.5, 1, 2, and 5C) was carried out by registering ten cycles for each current rate for R-LFP cell. The third program, needed to build the Ragone plot which delivers the energy versus power profile, was recorded for R-LFP and P-LFP at different constant power rates for one discharge then for one charge: 15, 10, 5, 2, and 1 W, with a potential window of 2–4 V.

Acknowledgements

The authors gratefully acknowledge the French National Research Agency (project Labex STORE-EX, ANR-10-LABX-76-01) for financial support. Dr. Carine Davoisne is wholeheartedly thanked for her precious help in recording the TEM images.

Conflict of Interest

The authors declare no conflict of interest.

Keywords: ascorbic acid • circular economy • green chemical lithiation • LiFePO₄ • lithium-ion batteries • regenerated 18650 cells • sustainability

- [1] D. Larcher, J.-M. Tarascon, *Nat. Chem.* **2015**, *7*, 19.
- [2] S. Dühnen, J. Betz, M. Kolek, R. Schmuck, M. Winter, T. S. Placke Dühnen, J. Betz, M. Kolek, R. Schmuck, M. Winter, T. Placke, *Small Methods* **2020**, *4*, 2000039.
- [3] Y. Ding, J. Fu, S. Zhang, X. He, B. Zhao, J. Ren, J. Zhong, Z. Liu, *Sep. Purif. Technol.* **2024**, *338*, 126551.
- [4] P. Molaiyan, S. Bhattacharyya, G. S. dos Reis, R. Sliz, A. Paoletta, U. Lassi, *Green Chem.* **2024**, *26*, 7508.
- [5] X. Qiu, C. Wang, L. Xie, L. Zhu, X. Cao, X. Ji, *J. Power Sources* **2024**, *602*, 234365.
- [6] L. Laffont, C. Delacourt, P. Gibot, M. Y. Wu, P. Kooyman, C. Masquelier, J. M. Tarascon, *Chem. Mater.* **2006**, *18*, 5520.
- [7] G. Chen, X. Song, T. J. Richardson, *Electrochim. Solid-State Lett.* **2006**, *9*, A295.
- [8] Z. Li, D. Zhang, F. Yang, *J. Mater. Sci.* **2009**, *44*, 2435.
- [9] G. Harper, R. Sommerville, E. Kendrick, L. Driscoll, P. Slater, R. Stolk, A. Walton, P. Christensen, O. Heidrich, S. Lambert, A. Abbott, K. Ryder, L. Gaines, P. Anderson, *Nature* **2019**, *575*, 75.
- [10] M. Wang, K. Liu, S. Dutta, D. S. Alessi, J. Rinklebe, Y. S. Ok, D. C. W. Tsang, *Renewable Sustainable Energy Rev.* **2022**, *163*, 112515.
- [11] S. Jiang, X. Li, Q. Gao, X. Lyu, S. N. Akanyange, T. Jiao, X. Zhu, *Sep. Purif. Technol.* **2023**, *324*, 124630.
- [12] Battery Report, Volta. Foundation, Revision: 2024040101 **2023**.
- [13] J. Yang, K. Zhou, R. Gong, Q. Meng, Y. Zhang, P. Dong, *J. Environ. Manage.* **2023**, *348*, 119384.
- [14] Y. Zhao, X. Yuan, L. Jiang, J. Wen, H. Wang, R. Guan, J. Zhang, G. Zeng, *Chem. Eng. J.* **2020**, *383*, 123089.
- [15] Y. Jung, J. Kim, Newsletters EU Battery Regulation to Enter Into Force in **2024**.
- [16] J. Kumar, R. R. Neiber, J. Park, R. A. Soomro, G. W. Greene, S. A. Mazari, H. Y. Seo, J. H. Lee, M. Shon, D. W. Chang, K. Y. Cho, *Chem. Eng. J.* **2022**, *431*, 133993.
- [17] X. Lai, Y. Huang, H. Gu, C. Deng, X. Han, X. Feng, Y. Zheng, *Energy Storage Mater.* **2021**, *40*, 96.
- [18] H. Bae, Y. Kim, *Mater. Adv.* **2021**, *2*, 3234.
- [19] M. Zhang, L. Wang, S. Wang, T. Ma, F. Jia, C. Zhan, *Small Methods* **2023**, *7*, 2300125.
- [20] B. Zhang, Y. Xu, D. S. Silvester, C. E. Banks, W. Deng, G. Zou, H. Hou, X. Ji, *J. Power Sources* **2024**, *589*, 233728.
- [21] D. D. S. Vasconcelos, J. A. S. Tenório, A. B. Botelho Jr, D. C. R. Espinosa, *Metals* **2023**, *13*, 543.
- [22] S.-H. Zheng, X.-T. Wang, Z.-Y. Gu, H.-Y. Lü, X.-Y. Zhang, J.-M. Cao, J.-Z. Guo, X.-T. Deng, Z.-T. Wu, R.-H. Zeng, X.-L. Wu, *J. Power Sources* **2023**, *587*, 233697.
- [23] X. Zhu, X. Ren, J. Chen, M. Gong, R. Mo, S. Luo, S. Yang, *Nanoscale* **2024**, *16*, 3417.
- [24] M. Fan, X. Chang, X. H. Meng, C. F. Gu, C. H. Zhang, Q. Meng, L. J. Wan, Y. G. Guo, *CCS Chem.* **2023**, *5*, 1189.
- [25] C. Li, R. Gong, Y. Zhang, Q. Meng, P. Dong, *Molecules* **2024**, *29*, 3340.
- [26] J. Yan, J. Qian, Y. Li, L. Li, F. Wu, R. Chen, *Adv. Funct. Mater.* **2024**, *34*, 2405055.
- [27] T. Ouaneche, M. Courty, L. Stievano, L. Monconduit, C. Guéry, M. T. Sougrati, N. Recham, *J. Power Sources* **2023**, *579*, 233248.

- [28] Q. Jing, J. Zhang, Y. Liu, W. Zhang, Y. Chen, C. Wang, *ACS Sustainable Chem. Eng.* **2020**, *8*, 17622.
- [29] T. Ouaneche, L. Stievano, L. Monconduit, C. Guéry, M. T. Sougrati, N. Recham, *Energy Storage Mater.* **2024**, *70*, 103507.
- [30] V. A. Timoshnikov, T. V. Kobzeva, N. E. Polyakov, G. J. Kontogiorghe, *Int. J. Mol. Sci.* **2020**, *21*, 3967.
- [31] L. Ling, *In Top. Chem. Mater. Eng.*, Volkson Press **2018**, *1*, pp. 21–23.
- [32] J. Chen, S. Wang, M. S. Whittingham, *J. Power Sources* **2007**, *174*, 442.
- [33] J.-M. Tarascon, N. Recham, M. Armand, J.-N. Chotard, P. Barpanda, W. Walker, L. Dupont, *Chem. Mater.* **2010**, *22*, 724.
- [34] K. Vediappan, A. Guerfi, V. Gariépy, G. P. Demopoulos, P. Hovington, J. Trottier, A. Mauger, C. M. Julien, K. Zaghib, *J. Power Sources* **2014**, *266*, 99.
- [35] N. Recham, M. Armand, L. Laffont, J.-M. Tarascon, *Electrochem. Solid-State Lett.* **2009**, *12*, A39.
- [36] C. Masquelier, P. Reale, C. Wurm, M. Morcrette, L. Dupont, D. Larcher, *J. Electrochem. Soc.* **2002**, *149*, A1037.
- [37] A. Bowino, G. Capannelli, S. Munari, S. Chimico-Fisici, S. Naturali, C. C. Industriale, **1988**, *26*, 785.
- [38] C. Delacourt, C. Wurm, P. Reale, M. Morcrette, C. Masquelier, *Solid State Ionics* **2004**, *173*, 113.
- [39] A. Padhi, K. S. Nanjundaswamy, J. B. D. Goodenough, *Journal of The Electrochemical Society* **1997**, *144*, 1188.
- [40] J. Wang, X. Sun, *Energy Environ. Sci.* **2012**, *5*, 5163.
- [41] I. Beyers, A. Bensmann, R. Hanke-Rauschenbach, *J. Energy Storage* **2023**, *73*, 109097.
- [42] Y. Bai, R. Essehli, C. J. Jafta, K. M. Livingston, I. Belharouak, *ACS Sustainable Chem. Eng.* **2021**, *9*, 6048.

Manuscript received: December 4, 2024

Revised manuscript received: March 10, 2025

Version of record online: March 11, 2025